LIQUID CRYSTALS, 1993, VOL. 15, NO. 1, 25–30

Optical properties of magnetically doped cholesterics

by YUVARAJ SAH, K. A. SURESH* and G. S. RANGANATH
Raman Research Institute, Bangalore 560080, India

(Received 4 October 1992; accepted 16 February 1993)

We have computed the optical diffraction pattern for linearly polarized light incident normal to the twist axis (phase grating mode) of a magnetically doped cholesteric (ferrocholesteric). The intrinsic Faraday rotation of the magnetic grains results in extra orders of diffraction. Also we find diffraction for any azimuth of the incident vibration. Further, using the Jones N matrices we have worked out the optical properties for light propagation along the twist axis on the very low wavelength side of the reflection band. We find that the medium behaves very differently from a normal cholesteric.

1. Introduction

Cholesteric phases in which magnetic grains are suspended have become important in recent times. Cholesteric phases of rod-shaped molecules in which needle-shaped magnetic grains are aligned along the local director have been realized in the laboratory. There are systems with grains having magnetization parallel to the local director [1] as well as magnetization perpendicular to the local director [2]. The former will give rise to a magnetically doped cholesteric (ferrocholesteric) phase with magnetization gradually twisting with the local director much like a helimagnetic system and in the latter case we get the same phase with the magnetization of the grains parallel to the twist axis. Since these grains can even be optically transparent (for example garnets), their inherent Faraday rotation becomes very important.

The rotatory power due to magnetic grains depends on the direction of propagation of light with respect to the magnetization m and is given by

$$\rho=\beta|\mathbf{m}|\cos\theta=\rho_0\cos\theta$$

where β is a constant and θ is the angle between m and the direction of propagation. This dependence of the Faraday rotation on θ leads to optical properties which are very different from those of the normal cholesterics. We have tried to bring out salient differences between the magnetically doped cholesterics (MDCs) and normal cholesterics.

In § 2 we have considered linearly polarized light propagating perpendicular to the twist axis (phase grating mode) of MDCs. The optical periodicity for such a medium is P, the pitch, instead of $P/2$ as in cholesterics. This modification of the periodicity gives rise to extra orders (odd orders) of diffraction in addition to those orders (even orders) obtained in cholesterics. In this sense the diffraction pattern is very similar to that of a S_C^* phase [3, 4].

In § 3 we have worked out the properties of the medium for light propagation along the twist axis, far away, on the lower wavelength side of the reflection band.

*Author for correspondence.

We find that depending upon the sign of optical rotation, the medium can act as a Mauguin retarder or a de Vries rotator.

2. Light propagation perpendicular to the twist axis

2.1. *Theory*

We consider the magnetization m of the grains to be parallel to the local director. We further assume that the medium is locally uniaxial about the local director. The linearly polarized light incident on the medium will see a variation of refractive index along Z, the twist axis, so that the incident plane wavefront emerges as a periodically corrugated wavefront with fluctuations in azimuth and ellipticity of the state of polarization. As linearly polarized light travels along any layer it splits into two orthogonal elliptic vibrations. The refractive indices of the medium for these two elliptic vibrations are given by [5]

$$\frac{1}{n_R^2}=\frac{1}{2}\left[(\eta_\perp(z)+\eta_\parallel(z))-\left|(\sqrt{[(\eta_\perp(z)-\eta_\parallel(z))^2+4\gamma^2]})\right|\right],$$

$$\frac{1}{n_L^2}=\frac{1}{2}\left[(\eta_\perp(z)+\eta_\parallel(z))+\left|(\sqrt{[(\eta_\perp(z)-\eta_\parallel(z))^2+4\gamma^2]})\right|\right],$$

where

$$\eta_\perp(z)=\frac{\cos^2(\alpha)}{n_1^2}+\frac{\sin^2(\alpha)}{n_2^2},$$

$$\eta_\parallel(z)=\frac{1}{n_1^2}.$$

Here $\alpha=(2\pi/P)z$, and n_2, n_1 are the refractive indices along and perpendicular to the local director in the absence of Faraday rotation.

The parameter γ is related to the rotatory power ρ of the medium by the relation

$$\gamma=\frac{\rho\lambda}{(\bar{n})^3\pi}.$$

Here λ is the wavelength of light and $\bar{n}$ is the mean refractive index of the medium.

These elliptic vibrations have ellipticity given by

$$\omega_R=\frac{1}{2}\tan^{-1}\left[\frac{2\gamma}{\eta_\parallel-\eta_\perp}\right] \quad \text{and} \quad \omega_L=\pi/2-\omega_R.$$

The elliptic vibration can be mathematically resolved at each point of the emergent wavefront into two linear vibrations polarized along and normal to the twist axis. This results in two periodically corrugated, orthogonally linearly polarized wavefronts given by

$$U_\parallel(z)=A_\parallel(z)\exp[i\psi_\parallel(z)],$$

and

$$U_\perp(z)=A_\perp(z)\exp[i\psi_\perp(z)],$$

where $A_\parallel(z)$ and $A_\perp(z)$ are the amplitude fluctuations and $\psi_\parallel(z)$ and $\psi_\perp(z)$ are the phase fluctuations of these wavefronts, respectively. We assume that the wavelength of the corrugation is large compared to its amplitude. The diffraction patterns due to these two wavefronts are given by their individual Fourier transforms. The complete diffraction pattern is obtained by coherently adding the diffraction pattern due to the two wavefronts.

2.2. Results and discussion

Using the above theory we have computed the diffraction pattern for experimentally realisable parameters.

The Faraday rotation due to the magnetic grains results in diffraction for any azimuth 4 (with respect to the twist axis) of the incident, linearly polarized light, unlike cholesterics where it occurs only for $0<\phi\leq\pi/2$. Also the MDC has a periodicity of 2π due to the magnetization m which will result in extra orders of diffraction. We find that for $\phi=0$ or $\pi/2$ the odd orders are linearly polarized in the state orthogonal to that of the incident light whereas the even orders are linearly polarized in the same state as that of the incident light. We also find that for any other general azimuth 4 in the range $0<\phi<\pi/2$ the odd and even orders are in general elliptically polarized.

The computed diffraction patterns with intensity as a function of scattering vector are shown in figures I (a), (b), 2(*a*) and (b). Each set gives patterns corresponding to a given value of the Faraday rotatory power ρ and for $\phi=0$, $\pi/4$ and $\pi/2$. We find the interesting result that the intensity of any odd order is independent of the azimuth of the incident light and only varies with ***p***. The Faraday

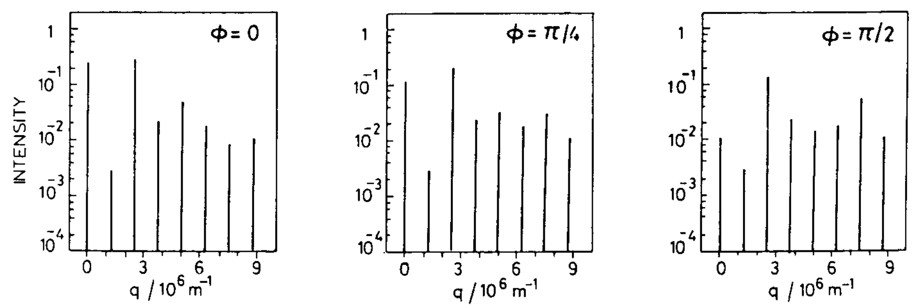

(*a*)

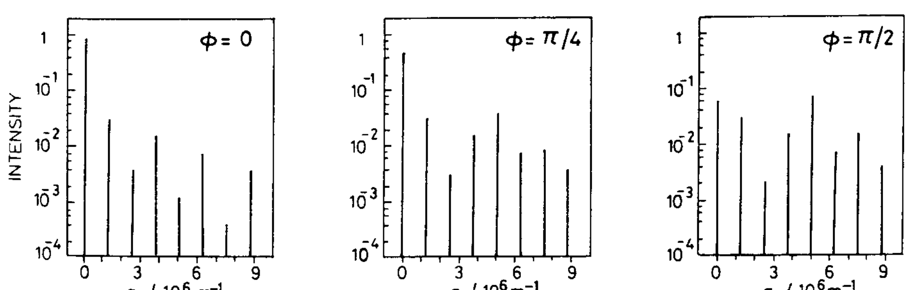

(*b*)

Figure 1. Computed diffraction pattern in a MDC showing intensity as a function of scattering vector q for $\lambda=0{\cdot}633\,\mu$m; $\Delta n=0{\cdot}07$; $n_1=1.535$; $n_2=1.605$; $P=5$ pm: sample thickness $(t)=20$ pm. For (a) $\rho_0=1.92\times10^{2}$ rad cm^{-1}, and for (b) $\rho_0=3{\cdot}84\times10^2$ rad cm^{-1}.

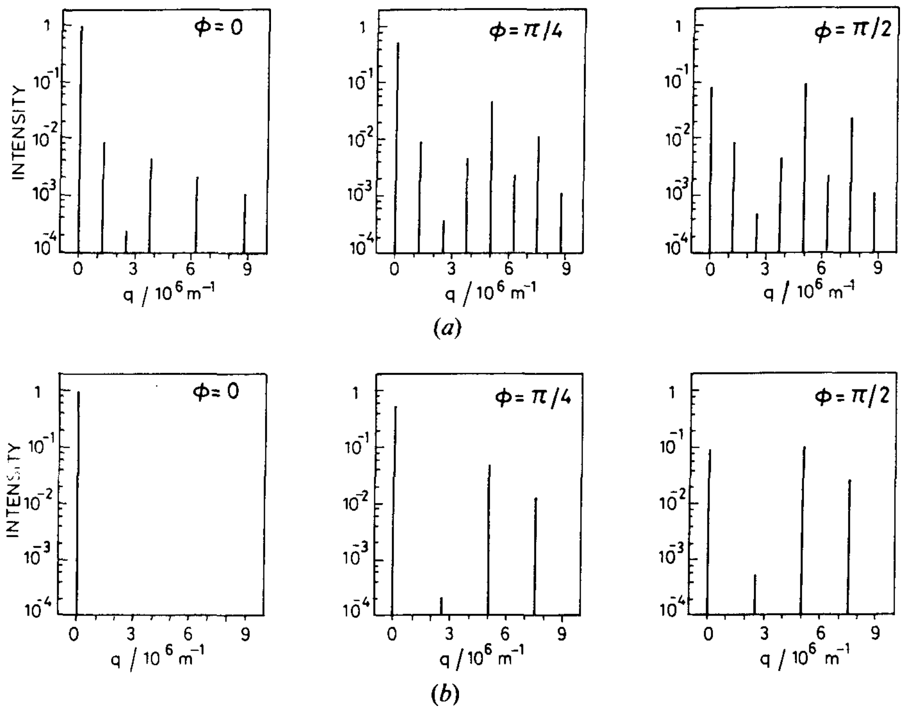

Figure 2. Computed diffraction pattern for the same values of λ, Δn, n_1, n_2, P and t given figure 1. For (*a*) $\rho_0 = 1.92 \times 10^2$ rad cm^{-1}, and for (*b*) $\rho_0 = 0$, i.e. a normal cholesteric.

rotation not only results in extra orders but also alters the intensities of the even orders as can be seen from the figures. All these features are seen even at extremely low values of ρ (see figure 2 (*a*)). It should be noted that in the diffraction patterns calculated for higher values of ρ, the intensities of the higher orders grow at the expense of lower orders (see figure 1 (a)). For comparison we give in figure 2(*h*) the diffraction patterns for zero Faraday rotation (i.e. a normal cholesteric). As is to be expected, in this case the odd orders do not exist at all for any value of ϕ and for $\phi = 0$ the entire pattern degenerates to the zeroth order. We would like to remark that in many respects the intensity and polarization features of the odd orders of diffraction pattern are very similar to those found for the S_C^* phase [3].

3. Light propagation parallel to the twist axis

3.1. *Theory*

In this case we assume that the magnetic grains are parallel to the local director but with m along the twist axis. The medium at any point acts as a linearly birefringent plate having Faraday rotation.

In the Jones matrix formulation, the N matrix for such a plate is given by [6]

$$\mathbf{N}_0 = \begin{bmatrix} -ik + ig_0 & -\rho \\ \rho & -ik - ig_0 \end{bmatrix},$$

where $2g_0$ is the phase retardation per unit thickness, k is the wave vector in the medium and p is the Faraday rotatory power. We assume the medium to be twisting along the Z axis. Then the N matrix of a layer at z is given by

$$\mathbf{N}=S(q_0z)\mathbf{N}_0S(-q_0z),$$

where $q_0=2\pi/P$,

$$S(q_0z)=\begin{bmatrix}\cos q_0z & -\sin q_0z\\ \sin q_0z & \cos q_0z\end{bmatrix}$$

so that the Jones M matrix for the entire sample can be written as

$$\mathbf{M}=S(q_0z)\exp[\{\mathbf{N}_0-q_0S(\pi/2)\}z].$$

If the electric vector of the incident light is

$$\mathbf{E}=\begin{bmatrix}E_x\\ E_y\end{bmatrix},$$

then the emergent electric vector is given by

$$\mathbf{E}'=\begin{bmatrix}E'_x\\ E'_y\end{bmatrix}=\mathbf{M}\begin{bmatrix}E_x\\ E_y\end{bmatrix}=\mathrm{ME}.$$

3.2. Results and discussion

3.2.1. Case I

$|\rho-q_0|\gg|g_0|$ with ρ and q_0 of opposite signs (i.e. when the direction of propagation of light is opposite to that of m). Then

$$\mathrm{M}=\exp(ikz)S(\rho z).$$

The medium, to a very good approximation, acts as a pure rotator, i.e. there will be a rotation in the plane of polarization of the incident light entering the medium.

3.2.2. Case 2

$|(\rho-q_0)|\ll|g_0|$ with ρ and q of the same sign (when the propagation of light is in the same direction as that of m). Then

$$\mathrm{M}=\exp(ikz)\begin{bmatrix}\cos q_0z & -\sin q_0z\\ \sin q_0z & \cos q_0z\end{bmatrix}\begin{bmatrix}\exp(ig_0z) & 0\\ 0 & \exp(-ig_0z)\end{bmatrix}.$$

This leads to Maugin's solution, i.e. the incident vibration splits into two linear orthogonal vibrations polarized along and perpendicular to the local director. As these vibrations travel they follow the director as in a twisted nematic.

Therefore depending on the propagation of light along or opposite to the direction of m the medium can act as a Mauguin retarder or as a de Vries rotator, respectively. For example, this happens for a MDC of pitch $\simeq 30\,\mu$m,. $\rho_0\simeq 2.0\times 10^3$ rad cm^{-1} and birefringence $An=0.025$. Such a medium between two appropriately aligned polaroids can act as an optical diode, i.e. transmitting light in one direction and blocking it completely in the opposite direction.

Interestingly, the condition $|(\rho-q_0)|\gg|g_0|$ need not imply that $|q_0|\gg|g_0|$. Here this condition can also be satisfied for small values of q_0, i.e. for large values of pitch. Thus the existance of Faraday rotation can lead to a de Vries limit even for a medium of large pitch. This is contrary to the case of normal cholesterics where the de Vries limit is reached only for very small pitch values.

Further the condition $|(\rho - q_0)| \ll |g_0|$ does not mean that $|q_0| < |g_0|$. In fact $|q_0| > |g_0|$ is also possible. In this situation, in the absence of Faraday rotation, the solution will not go over to Mauguin's limit, but to the de Vries limit [7].

The authors would like to thank Sunil Kumar for discussions. Our thanks are also due to the referee for suggestions.

References

[1] RAULT, J., CLADIS, P. E., and BURGER, J. P., **1970,** ***Physics Lett.* A, 32, 199.**
[2] CHEN, S. H., and AMER, N. M., **1983,** ***Phys. Rev. Lett.*, 51, 2298.**
[3] SURESH, K. A., SUNIL KUMAR, P. B., and RANGANATH, G. S., **1992,** ***Liq. Crystals*, 11, 73.**
[4] JOHNSON, R. V., and TANGUAY, A. R., **1986,** ***Opt. Engng*, 25, 235.**
[5] RAMACHANDRAN, G. N., and RAMASESHAN, S., **1961,** ***Handbuch der Physik*, Vol. 25,** Part 1 (Springer Verlag), p. **81.**
[6] JONES, R. C., **1948,** ***J. opt. Am.*, 33, 671.**
[7] CHANDRASEKHAR, S., RANGANATH, G. S., KINI, U. D., and SURESH, K. A., **1973,** ***Molec. Crystals liq. Crystals*, 24, 202.**

Anomalous transmission at oblique incidence in absorbing cholesteric liquid crystals

Yuvaraj Sah and K. A. Suresh

Raman Research Institute, Bangalore 560080, India

Received April 8, 1993; revised manuscript received July 26, 1993; accepted July 29, 1993

We consider theoretically light propagation at oblique incidence in absorbing cholesteric liquid crystals in the Bragg mode. Using 2×2 matrix procedure, we analyze the eigenmodes in terms of the forward- and backward-propagating eigenwaves inside the isotropic medium bounding the cholesteric liquid crystal. The nature of the eigenmodes in the medium changes continuously from the circular to the linear state with increase in the angle of incidence. Using the appropriate eigenmodes, we studied anomalous transmission in first and second Bragg orders in these systems and its relevance to the reported experimental results. We find some interesting polarization features that arise as a result of the absorption in the cholesteric medium.

INTRODUCTION

The cholesteric liquid crystalline phase (cholesterics) has a locally birefringent structure that twists uniformly about a particular direction. The optical properties of cholesterics have been studied extensively both theoretically and experimentally.[1–5] The helical structure of the phase gives rise to many interesting optical properties, namely, selective Bragg reflections, non-Bragg total reflection, and anomalous transmission in absorbing cholesterics.

Anomalous transmission at normal incidence has been studied theoretically and confirmed experimentally.[6–8] A related effect at oblique incidence was studied by Endo *et al.*[9] These authors found that anomalous transmission occurs only at small angles of incidence, i.e., below 19°.

Here we undertake theoretical studies on light propagation at oblique incidence in absorbing cholesterics that are aligned in planar geometry (the twist axis perpendicular to the sample plane). Our computations show that the nature of the eigenmodes inside the isotropic medium bounding the cholesteric changes gradually from circular to linear as we increase the angle of incidence. Since the polarization of the eigenmodes changes with the angle of incidence, one must choose an incident wave with proper polarization to observe anomalous transmission. This is the main reason that Endo *et al.*[9] did not observe the effect experimentally at large angles of incidence.

It is well known that higher-order reflection bands occur when light is incident obliquely to the planar cholesteric.[10–12] We have also worked out the effect of absorption on the second-order reflection band.

THEORY

According to Oseen's model of cholesterics, the dielectric tensor for the cholesteric is given by

$$\varepsilon = \begin{bmatrix} \varepsilon + \delta \cos 2\beta z & \delta \sin 2\beta z & 0 \\ \delta \sin 2\beta z & \varepsilon - \delta \cos 2\beta z & 0 \\ 0 & 0 & \varepsilon_2 \end{bmatrix}.$$

$\varepsilon = (\varepsilon_1 + \varepsilon_2)/2$, $\delta = (\varepsilon_1 - \varepsilon_2)/2$, and $\beta = 2\pi/P$, where P is the pitch of the medium and ε_1 and ε_2 are the principal values of the dielectric tensor.

In Berreman's 4×4 matrix formulation[13] Maxwell's equations can be written as

$$\frac{\partial \psi(z)}{\partial z} = \frac{i\omega}{c} \Delta(z) \psi(z), \tag{1}$$

where

$$\psi(z) = \begin{bmatrix} E_x \\ H_y \\ E_y \\ -H_x \end{bmatrix}.$$

$\Delta(z)$ is a 4×4 matrix that is periodic in z. E_x, E_y and H_x, H_y are the x and the y components of the electric and magnetic fields, respectively, with z being the propagation direction.

Equation (1) can be solved numerically for one pitch to produce the propagation matrix $F(z, P)$ for the cholesteric medium. $F(z, P)$ relates the field at the point $(z + P)$ to the field at z given by

$$\psi(z + P) = F(z, P)\psi(z). \tag{2}$$

The eigenvectors ξ_j (where $j = 1, 2, 3,$ and 4) of $F(z, P)$ correspond to the eigenfields of the four eigenmodes (two forward and two backward modes). The eigenfield of the particular eigenmode at any point z_1 situated at an infinitesimal distance h from z can be obtained by

$$\xi_j(z_1) = \exp\left[i \frac{\omega}{c} \Delta(z) h\right] \xi_j(z). \tag{3}$$

In computing the total intensity of the E field inside the medium for the obliquely incident light, we have also considered the z component of the E field. The transmittance and reflectance for incident waves of different polarization are computed with use of the propagation matrix for an integral number of pitches.

In an experimental situation the cholesteric is sandwiched between two glass plates (isotropic medium). It is

0740-3232/94/020740-05$06.00

convenient to analyze the transmitted and reflected waves in terms of the forward- and backward-propagating modes inside the bounding isotropic medium. We use Oldano's transformation matrix T (Ref. 14) for the transverse magnetic (TM) and transverse electric (TE) polarizations (with respect to the plane of incidence) to analyze the reflected and transmitted waves. We employ a 2×2 matrix procedure[15] to analyze the eigenmodes in the cholesteric medium (bounded by the glass plates).

One can write at the first glass–cholesteric interface,

$$\Psi(z) = T\phi_I(z), \tag{4}$$

where

$$\phi_I(z) = \begin{bmatrix} i_1 \\ i_2 \\ r_1 \\ r_2 \end{bmatrix},$$

and at the second interface,

$$\psi(z + nP) = T\phi_I(z + nP), \tag{5}$$

where

$$\phi_I(z + nP) = \begin{bmatrix} t_1 \\ t_2 \\ 0 \\ 0 \end{bmatrix}.$$

Here i_1, i_2 are the incident, r_1, r_2 are the reflected, and t_1, t_2 are the transmitted amplitudes of the TM and the TE waves, respectively, inside the isotropic medium, the number of pitches in the cholesteric medium being n.

Using Eq. (2) and the property of the propagation matrix $F(z, nP) = [F(z, p)]^n$, for n pitches one can write that

$$\psi(z) = F^{-1}(z, nP)\psi(z + nP). \tag{6}$$

Using Eqs. (4)–(6), we get

$$\phi_I(z) = C\phi_I(z + nP), \tag{7}$$

where $C = T^{-1}F^{-1}(z, nP)T$.

With use of Eq. (7) it follows that

$$\begin{bmatrix} t_1 \\ t_2 \end{bmatrix} = D_1\begin{bmatrix} i_1 \\ i_2 \end{bmatrix}, \qquad \begin{bmatrix} r_1 \\ r_2 \end{bmatrix} = D_2\begin{bmatrix} i_1 \\ i_2 \end{bmatrix}. \tag{8}$$

The eigenvectors of D_1 and D_2 represent the forward- and the backward-propagating eigenmodes, respectively, in the isotropic medium. These eigenmodes in the isotropic medium bounding the cholesteric give us the waves that are responsible for forming the standing and the propagating waves inside the cholesteric medium. For example, at normal incidence the eigenvectors of D_1 and D_2 are orthogonal circular waves. The resultant vibrations of these waves gives rise to the linearly polarized standing waves with E$\|$H (Ref. 15) and a propagating circular wave. At high angles of incidence these eigenwaves are linearly polarized. It is interesting to note that these eigenwaves are similar to the eigenwaves inside the cholesteric medium calculated by Miraldi *et al.*,[16] which are circular at normal incidence and predominantly linear at large angles of incidence. From Eq. (8) one can also compute the reflectance and the transmittance for TM and TE waves.

RESULTS AND DISCUSSION

Throughout, we have assumed a right-handed cholesteric medium. In our calculations we have chosen $\varepsilon_1 = 2.3228 + i \times 0.0063$ and $\varepsilon_2 = 2.5673 + i \times 0.063$ for the absorbing cholesteric medium. The reflectance and transmittance were computed for 25 pitches for different values of P/λ, where λ is the wavelength of light.

First-Order Bragg Reflection

When the right circularly (RC) polarized wave is incident normally upon a planar-aligned cholesteric, it experiences enhanced transmission[8] in the short-wavelength side of the Bragg band compared with the left circularly (LC) polarized wave. The LC wave does not sense the helical structure and hence experiences the average absorption of the medium. Endo et *al.*[9] used RC and LC waves and found that the anomalous transmission occurs only at small angles. Since at these small angles the eigenmodes deviate very little from the circular state, anomalous transmission can be observed. For angles of incidence $\theta > 30°$ the circular waves are no longer the eigenmodes. Hence using these waves at large angles is not appropriate while one is performing anomalous-transmission experiments. One has to choose the proper polarization of the incident wave, which is the same as that of the eigenmode of D_1, to observe anomalous transmission. At intermediate angles (30–55°) the eigenvectors of D_1 and D_2 matrices depend on λ even within the reflection band and are in general elliptic. Experimental observation of the effect at these angles can be difficult, as the nature of the polarization of the eigenmodes varies with both angle and wavelength.

For large angles of incidence the eigenvectors of D_1 and D_2 matrices are predominantly linear, and the nature of the eigenmode does not change within the reflection band. At these large angles for nonabsorbing cholesteric, the Bragg band splits into three subbands. One can use the TE and TM waves that are the eigenvectors of D_1 and D_2 to study anomalous transmission in the absorbing cholesteric medium. The propagation of the TE and TM waves in the absorbing cholesterics is such that in the short-wavelength region the TM wave that is reflected more also shows an enhanced transmission. This is shown in Figs. 1 and 2.

We have calculated the dependence of reflectance and transmittance on the angle between the plane of incidence and the director (major principal axis of the dielectric tensor) of the cholesteric layer at the boundary. We find that the dependence of the transmittance on this angle is almost negligible, whereas the dependence of the reflectance is pronounced, particularly for TE–TE polarization as shown in Fig. 3.

In nonabsorbing cholesterics in the non-Bragg reflection region, the reflectance is always unity and is independent of the polarization of the incident light. Our results show that in the absorbing case the reflectivity in this region is highly dependent on the state of polarization of the incident light. One can understand this dependence of the reflectance on polarization by looking at the intensity of the electric field of the nonpropagating eigenmodes computed from Berreman's 4×4 matrices.[13] In the absence of absorption the fields of the two nonpropagating eigenmodes suffer attenuation to the same extent

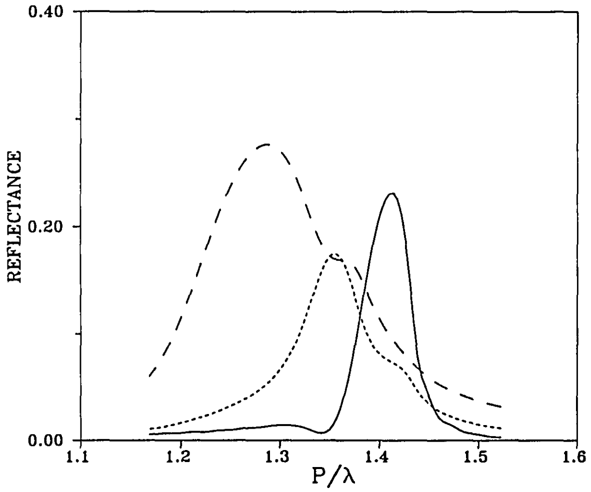

Fig. 1. Reflectance of TM–TM (solid curve), TE–TM (short-dashed curve), TE–TE (long-dashed curve) waves for an absorbing cholesteric at 8 = 60°.

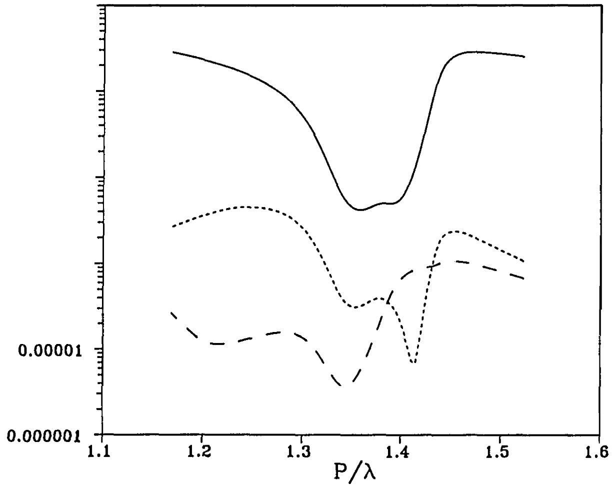

Fig. 2. Transmittance of TM–TM (solid curve), TE–TM (short-dashed curve), and TE–TE (long-dashed curve) waves for an absorbing cholesteric at 8 = 60°.

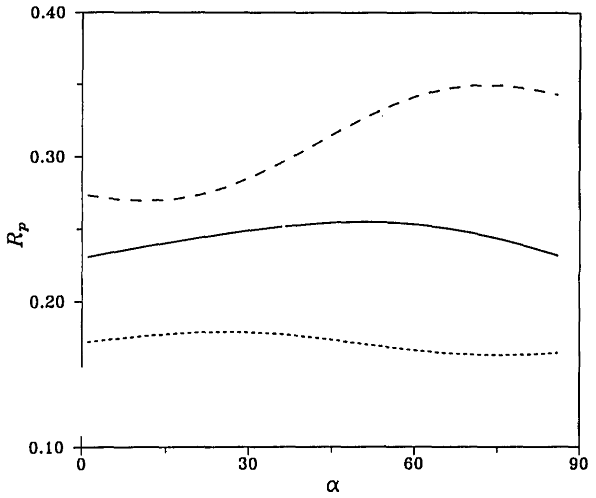

Fig. 3. Peak reflectance (R_p) for TM–TM (solid curve), TM–TE (short-dashed curve), and TE–TE (long-dashed curve) as a function of α (in degrees), the angle between the plane of incidence and the director of the cholesteric layer at the boundary.

(see Fig. 4). But in the presence of absorption, the two eigenmodes experience the absorption of the medium differently and one eigenmode gets attenuated more than the other. Hence the reflectance becomes polarization dependent.

Second-Order Bragg Reflection

In the nonabsorbing cholesteric, as in the first-order reflection, the second order reflection also has three subbands. We find that in the absorbing cholesteric the TM wave experiences less attentuation throughout the band and is transmitted more than the TE wave. In fact, the transmittance is almost zero for the TE wave (see Fig. 5). For comparison, the reflectance for TE and TM waves is shown in Fig. 6. We find that in this order the anomalous transmission for the TM wave that occurs at the short-wavelength region is not so pronounced as it is in the first Bragg order.

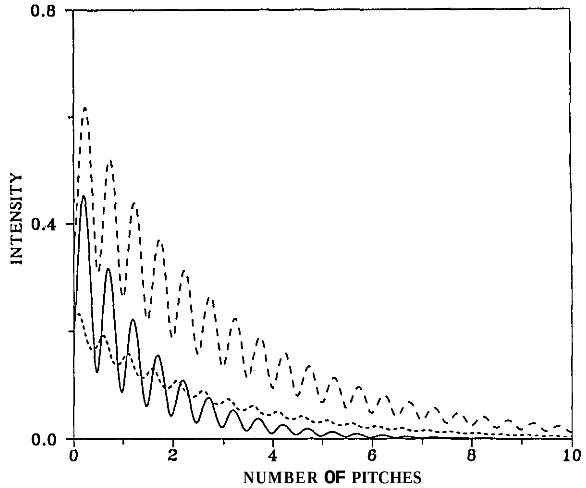

Fig. 4. Intensity of the E field of the two nonpropagating modes in the non-Bragg region for nonabsorbing (long-dashed curve) cholesteric as a function of number of pitches (in this case the two modes are attenuated by the same amount) and the intensity of the E field for the same two modes (solid and short-dashed curves) in the same region for the absorbing cholesteric medium at $\theta = 60°$.

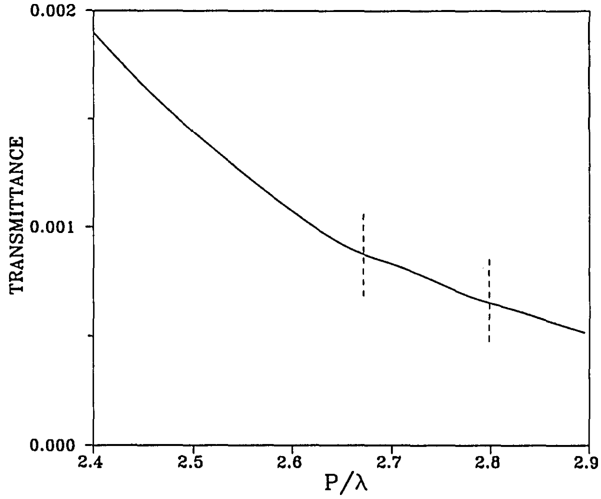

Fig. 5. Transmittance of TM (solid curve) wave for an absorbing cholesteric at $\theta = 60°$ in the second-order Bragg reflection. The dashed vertical lines indicate the region of anomalous transmission. Here the transmittance for the TE wave is almost zero.

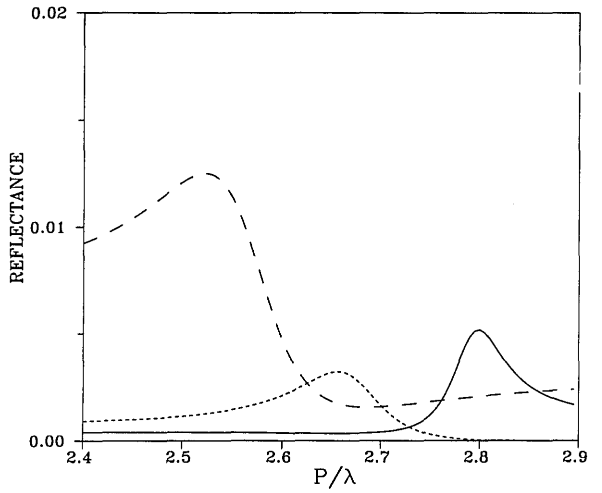

Fig. 6. Reflectance of TM–TM (solid curve), TE–TM (short-dashed curve), TE–TE (long-dashed curve) waves for an absorbing cholesteric at 8 = 60° in the second-order Bragg reflection.

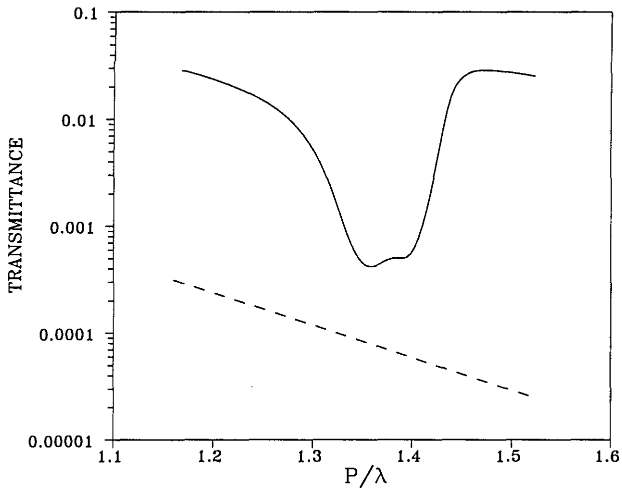

Fig. 7. Transmittance of TM wave (solid curve) at 8 = 60°. The dashed line represents the transmittance of the same wave through a medium that has an absorption coefficient given by $[\mathrm{Im}(\sqrt{\varepsilon_1}) + \mathrm{Im}(\sqrt{\varepsilon_2})]/2$ for the same 8.

Optical Analogue of the Borrmann Effect

We now consider the optical analogue of an interesting effect in x-ray diffraction of crystals. X rays incident upon a nonabsorbing crystal set at the Bragg angle undergo reflection, and hence the transmitted wave suffers attenuation. When an absorbing crystal is at the Bragg setting one expects further attenuation in the transmitted wave. Borrmann found an enhanced transmission that was more than the transmission that is due to average absorption alone of the crystal not at the Bragg setting. This phenomenon of anomalous transmission is called the Borrmann effect.[17]

In the optical region, for absorbing cholesterics the RC and LC waves incident normally upon a planar cholesteric are the eigenwaves. Here the LC wave does not experience the structure, and it experiences average absorption. Hence the anomalous transmission of the RC wave can be compared with the LC wave, and it is a clear analogue of the Borrmann effect in x rays. At high angles of incidence both eigenwaves, TE and TM, experience the structure, and therefore the transmitted intensity of these waves cannot be compared analogously with the Borrman effect. Therefore we take a value of the absorption coefficient equal to $[\mathrm{Im}(\sqrt{\varepsilon_1}) + \mathrm{Im}(\sqrt{\varepsilon_2})]/2$ that is experienced by the LC wave at normal incidence. Using this value, we calculate the transmittance at oblique incidence for the TM waves through an isotropic medium. This is analogous to the transmittance of the x rays through an absorbing crystal not at the Bragg setting. We compare this transmittance with the transmittance of the TM wave through the cholesteric medium and bring out the analogy with the Borrmann effect. We find that the TM wave is anomalously transmitted over the entire Bragg band, exhibiting the Borrmann effect (see Fig. 7). This effect is also found in the second-order Bragg reflection.

Anomalous transmission at oblique incidence is sensitive to the polarization of the incident light. Also, at large angles when a TM wave is incident upon a planar cholesteric, anomalous transmission occurs in the short-wavelength region of the Bragg band. Only careful experimental studies on absorbing cholesterics at oblique incidence will give more insight into the phenomenon of anomalous transmission.

ACKNOWLEDGMENTS

We thank G. S. Ranganath and P. B. Sunil Kumar for many useful discussions. Our thanks also to the referees for helpful suggestions.

REFERENCES

1. V. A. Belyakov and V. D. Dmitrienko, "Theory of the optical properties of cholesteric liquid crystals," Sov. Phys. Solid State 15, 1811–1815 (1974).
2. C. Oldano, E. Miraldi, and P. T. Valabrega, "Dispersion relation for propagation of light in cholesteric liquid crystals," Phys. Rev. A 27, 3291–3299 (1983).
3. C. Oldano, "Many-wave approximation for light propagation in cholesteric liquid crystals," Phys. Rev. A 31, 1014–1021 (1985).
4. H. L. Ong, "Wave propagation in cholesteric and chiral smectic C liquid crystals: exact and generalized geometrical-optics approximation," Phys. Rev. A 37, 3520–3529 (1988).
5. H. Takezoe, Y. Ouchi, M. Hara, A. Fukuda, and E. Kuze, "Experimental studies of reflection spectra in monodomain cholesteric liquid crystal cell: total reflection, subsidiary oscillation and its beats or swell structure," Jpn. J. Appl. Phys. 22, 1080–1091 (1983).
6. R. Nityananda, U. D. Kini, S. Chandrasekhar, and K. A. Suresh, 'Anomalous transmission (Borrmann effect) in absorbing cholesteric liquid crystals," in Proceedings of the International Liquid Crystal Conference, Bangalore, December 3–8, 1973, Pramana Suppl. 1,325–340 (1975).
7. S. Chandrasekhar, G. S. Ranganath, and K. A. Suresh, "Dynamical theory of reflection from cholesteric liquid crystals," in Proceedings of the International Liquid Crystal Conference, Bangalore, December 3–8, 1973, Pramana Suppl. 1, 341–352 (1975).
8. K. A. Suresh, "An experimental study of anomalous transmission (Borrmann effect) in absorbing cholesteric liquid crystals," Mol. Cryst. Liquid Cryst. 35, 267–273 (1976).
9. S. Endo, T. Kuribara, and T. Akahane, 'A study of the anomalous transmission (Borrmann effect) on obliquely incident light in an absorbing single-domain cholesteric liquid crystal," Jpn. J. Appl. Phys. 22, L499–L501 (1983).
10. V. D. Dmitrienko and V. A. Belyakov, "Higher orders of selective reflection of light by cholesteric liquid crystals," Sov. Phys. Solid State 15, 2365–2366 (1974).

11. D. W. Berreman and T. J. Scheffer, "Bragg reflection of light from single-domain cholesteric liquid crystal films," Phys. Rev. Lett. **25,** 577–581 (1970).
12. H. Takezoe, K. Hashimoto, Y. Ouchi, M. Hara, A. Fukuda, and E. Kuze, "Experimental study on higher order reflection by monodomain cholesteric liquid crystal," Mol. Cryst. Liquid Cryst. **101,** 329–340 (1983).
13. D. W. Berreman, "Optics in stratified and anisotropic media: 4 × 4-matrix formulation," J. Opt. Soc. Am. **62,** 502–510 (1972).
14. C. Oldano, "Electromagnetic wave propagation in anisotropic stratified media," Phys. Rev. A **40,** 6014–6020 (1989).
15. P. B. Sunil Kumar and G. S. Ranganath, "Structure and optical behavior of cholesteric soliton lattices," J. Phys. II France **3,** 1497–1510 (1993).
16. E. Miraldi, C. Oldano, P. I. Taverona, and L. Trossi, "Optical properties of cholesteric liquid crystal at oblique incidence," Mol. Cryst. Liquid Cryst. **103,** 155–176 (1983).
17. R. W. James, The Optical Principles of the Diffraction of X-rays (Bell, London, 1967).

Optical Diffraction in Chiral Smectic-*C* Liquid Crystals

K. A. Suresh, Yuvaraj Sah, P. B. Sunil Kumar, and G. S. Ranganath
Raman Research Institute, Bangalore 560080, India
(Received 17 September 1993)

We report a study on the optical diffraction for light propagation perpendicular to the twist axis in the chiral smectic-C liquid crystal. In this phase grating mode, we find very unusual intensity and polarization features in the diffraction pattern. These observed features can be explained by invoking the theory of anisotropic gratings which takes into account the internal diffractions.

PACS numbers: 42.70.Df, 42.25.Fx

The chiral smectic-C (S_{C^*}) liquid crystal phase has a helical stack of layers of uniformly tilted molecules. The tilt of the molecules is coupled to the layer thickness producing local biaxiality in the medium. The chirality in the medium removes the mirror symmetry in the system leading to the possibility of sustaining an electric polarization P (along the local twofold axis), spiraling uniformly about the twist axis of the helical structure. Meyer *et* al. [1] discovered the existence of ferroelectricity in S_{C^*}. Technologically, S_{C^*} became very important after Clark and Lagerwall [2] demonstrated the submicrosecond dynamics and other related properties like symmetric bistability, threshold behavior, and large electro-optic response that are exploited in the fast switching display devices. Further, studies on pyroelectricity [3], shear induced polarization [4], electroclinic effect [5], second harmonic generation [6], and other phenomena [7] have established the rich physical properties exhibited by S_{C^*}. In addition, S_{C^*} has many interesting optical properties. These arise due to the fact that in the successive layers, the local index ellipsoid (triaxial ellipsoid) spirals uniformly about the twist axis at a constant angle. The study of propagation of light in the Bragg reflection mode has shown some distinct optical polarization properties peculiar to this phase [8–11]. The study of propagation of light perpendicular to the twist axis is equally interesting, but has drawn very little attention. In this geometry, the medium acts as a phase grating; i.e., a plane wave front incident on the sample becomes a periodically corrugated wave front inside the medium resulting in optical diffraction. So far, optical studies in this geometry have been largely confined to the determination of the pitch of the structure [12]. We have undertaken a study of the propagation of light in S_{C^*} in the phase grating mode in all its details.

In this Letter, we report for the first time some unusual features of diffraction associated with the phase grating mode in S_{C^*}. We observed that in a range of sample thicknesses, the diffracted light in all the orders was preferentially polarized parallel to the twist axis. Further, in thicker samples, although the above features were seen at lower temperatures, at higher temperatures the diffracted light in all the orders was nearly polarized perpendicular to the twist axis. These observed features contradict the predictions of the Raman-Nath theory of phase gratings [13] as extended to S_{C^*} [14] where the wave front corrugations inside the medium are ignored. It is shown here that a rigorous theory of anisotropic dielectric gratings as developed by Rokushima and Yamakita (RY) [15] can account for our observed features.

The experiments were carried out on the commercially obtained sample BDH SCE-6. This has the following sequence of transitions:

$$\text{Crystal} \underset{-15°\text{C}}{\rightarrow} S_{C^*} \underset{63°\text{C}}{\leftrightarrow} \text{Smectic-A} \underset{84°\text{C}}{\leftrightarrow} \text{Cholesteric} \underset{120°\text{C}}{\leftrightarrow} \text{Isotropic}$$

To get monodomain samples suitable for phase grating geometry, the following procedure was employed: Sample cells were prepared using glass plates which were previously treated with polyimide and rubbed in the parallel direction. Cells of thicknesses 23, 50, 125, and 250 μm were obtained using Mylar spacers. Later, the cells were filled with the sample in the isotropic phase and then cooled very slowly through the cholesteric to smectic-A (S_A) phase in the presence of a magnetic field of strength 2.4 T applied parallel to the rubbed direction of the glass plates. In the S_A phase, the field was removed. Observations under a Leitz polarizing microscope revealed the formation of a very good homogeneous monodomain S_A phase which on further slow cooling transformed to the S_{C^*} phase. In S_{C^*} we got a pattern having uniform parallel striations (fringes). The striations were perpendicular to the rubbed direction of the glass plates and were parallel to the smectic layers. They arise due to a uniformly twisted stack of layers (of tilted molecules) with the twist axis along the rubbed direction. The fringe width corresponds to the pitch of the helical structure [12]. In SCE-6, the pitch varies from about 4 to 6 μm in the temperature range of 25 °C to 60 °C. For samples of thicknesses much lower than 23 μm, due to the surface effects, the helical structure got considerably distorted and hence was not used. In the experimental setup, the cell was kept on the central table of a goniometer which had a 2 mW He-Ne laser (λ =0.6328 μm) on the fixed arm. The light was allowed to fall normally on the sam-

0031-9007/94/72(18)/2863(4)$06.00

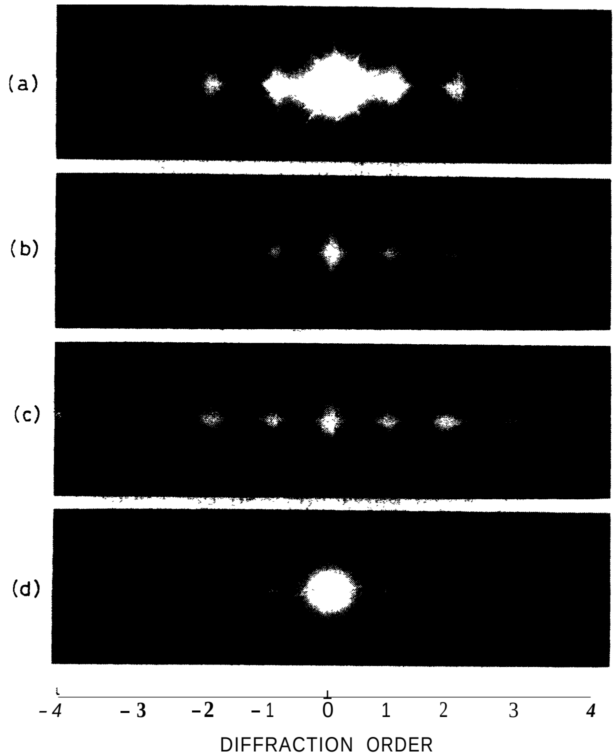

FIG. 1. The photographs of the diffraction pattern of a 50 μm sample at room temperature ($\approx 25\,°C$) in (a) HH, (b) HV, (c) VH, and (d) VV geometries. One may note that in (c) the second order is more intense than the first order. Such effects are characteristic of phase gratings. In S_{C*}, they are sensitive to temperature.

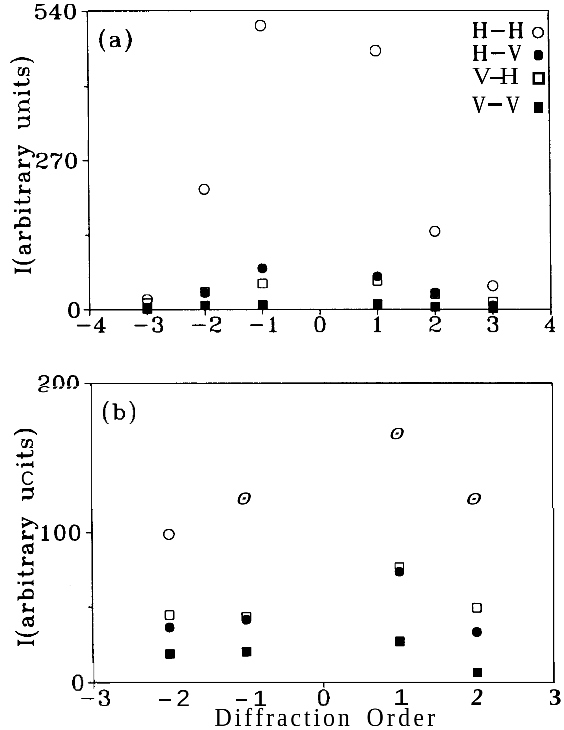

FIG. 2. The intensity I (arbitrary units) in the diffraction orders shown for various geometries for two samples: (a) thickness = 50 μm and temperature = 50.6 °C; (b) thickness = 250 μm and temperature = 45.5 °C. Here one may notice that in every order $I(HH) > I(HV)$ and $I(VH) > I(VV)$. The intensity of the direct beam is too high to be shown here. The asymmetry in the intensity pattern for some orders is due to slight imperfections in the orientation of the sample.

ple cell. The diffracted light was collected on a photodiode mounted on the moving arm and measured with a Keithley 181 nanovoltmeter. Simultaneously the signal was fed into a Graphtec servocorder.

In our experiments, for incident linearly polarized light, we got sharp diffraction spots. Typically there were 6 to 7 orders on either side of the direct beam. Figure 1 shows one such diffraction pattern in the geometries HH, HV, VH, and VV. (H denotes linear polarization parallel to the twist axis and V denotes linear polarization perpendicular to the twist axis. The first symbol indicates the state of polarization of the incident light and the second symbol indicates the polarization state in which the diffracted beam was analyzed.)

Figure 2 shows the measured diffracted intensity in the various orders (except the zeroth order) for 50 and 250 μm sample thicknesses. Surprisingly, the intensity in the HH geometry (open circles) is very much higher than the intensity in the HV geometry (closed circles) for all orders. Also the intensity in the VH geometry (open squares) is higher than that in the VV geometry (closed squares). That is, in all these orders, the diffracted light is nearly linearly polarized parallel to the twist axis. Interestingly, this behavior is observed in samples of thickness 23 and 50 μm at all temperatures. For 125 μm the same behavior is also seen at all temperatures except in the neighborhood of the S_{C*}-S_A transition. However, in the sample with a thickness of 250 μm, a more interesting behavior is found. At temperatures $\lesssim 46\,°C$ the intensity and polarization features are the same as that described above, But at higher temperatures, the behavior gets completely reversed. This is shown in Fig. 3. Here the intensity of the diffracted light in the VV geometry becomes more intense than the intensity in the VH geometry. Also the intensity in the HV geometry is more than that in the HH geometry: i.e., in this case, in all these orders, the component of the diffracted light perpendicular to the twist axis is more than the component parallel to the twist axis. However, in all these geometries, in all the samples, the zeroth order is in a polarization state close to that of the incident vibration. We have shown data on two samples [Figs. 2(a) and 3] of different thicknesses (50 and 250 μm) but at the same temperature (50.6 °C) to highlight their contrasting behavior.

The above results cannot be accounted for by the theory [14] of the optical diffraction in S_{C^*} which assumes that in the corrugated wavefront, inside the medium, the amplitude of the corrugation is much smaller than the wavelength of the corrugation; i.e., the internal diffractions are ignored. This assumption is valid only in the limit of low birefringence and small thickness. However, in the present case, the material has a high birefringence and the sample thicknesses are large. Hence we have used a more rigorous theory of anisotropic dielectric gratings due to RY [15] which incorporates the internal diffractions within the medium.

Following RY [15] and Galatola, Oldano, and Sunil Kumar [16], the Maxwell equations are written in the form

$$\Psi(z)=\exp(ik_0zD)\Psi(0)\,, \tag{1}$$

where

$$\Psi=(E_xH_yE_yH_z)^t$$

and

$$k_0=2\pi/\lambda\,.$$

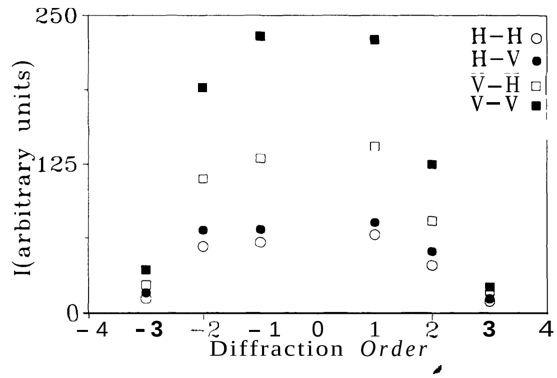

FIG. 3. The intensity I (arbitrary units) in the diffraction orders shown for various geometries for a 250 μm sample at 50.6 °C. One may notice that in every order $I(HH)<I(HV)$ and $I(VH)<I(VV)$.

E_x, E_y, H_x, and H_y are infinite column matrices containing the various Fourier components of the transverse fields and λ is the wavelength of light. The propagation matrix D for our problem simplifies to an infinite square matrix:

$$D=\begin{bmatrix} 0 & I & 0 & 0 \\ \varepsilon_{xx}-\varepsilon_{xz}\varepsilon_{zz}^{-1}\varepsilon_{xz}-Q^2 & 0 & \varepsilon_{xy}-\varepsilon_{xz}\varepsilon_{zz}^{-1}\varepsilon_{zy} & -\varepsilon_{xz}\varepsilon_{zz}^{-1}Q \\ -Q\varepsilon_{zz}^{-1}\varepsilon_{zx} & 0 & -Q\varepsilon_{zz}^{-1}\varepsilon_{zy} & I-Q\varepsilon_{zz}^{-1}Q \\ \varepsilon_{yx}-\varepsilon_{yz}\varepsilon_{zz}^{-1}\varepsilon_{zx} & 0 & \varepsilon_{yy}-\varepsilon_{yz}\varepsilon_{zz}^{-1}\varepsilon_{zy} & -\varepsilon_{yz}\varepsilon_{zz}^{-1}Q \end{bmatrix}$$

Here, ε_{xz}, etc. are themselves infinite square matrices. The ijth element of the matrix ε_{xz}, etc. is the $(i-j)$th Fourier component of the ε_{xz}, etc. element of the dielectric tensor ε. Q is an infinite diagonal matrix with elements q_0+nq, where q_0 is the incident wave vector in the bounding isotropic medium and q is the grating wave vector with n going from $-\infty$ to ∞; I is the infinite unit matrix.

To compare the theory with the experimental results it is convenient to work in terms of the modes in the bounding isotropic media. If @ is a vector whose components are the strengths of the different modes in the bounding isotropic media, then Eq. (1) becomes

$$\Phi(z)=S\Phi(0)\,, \tag{2}$$

where S is the scattering matrix whose components are functions of the material parameters. The vector $\Phi(0)$ contains the reflected Φ_r and incident Φ_i components, while $\Phi(z)$ contains the transmitted component Φ_t [16]. A suitable rearrangement in the elements of the Φ vector leads to

$$\Phi_r=\mathcal{R}\Phi_i,\quad \Phi_t=\mathcal{T}\Phi_i\,, \tag{3}$$

where $\mathcal{R}$ and $\mathcal{T}$ are the backward and forward scattering matrices, respectively.

It was sufficient to have the Fourier components up to $n=5$ in the dielectric tensor and also to assume local uniaxiality. Computations with higher Fourier components and biaxiality did not alter our main results. Figure 4 shows the computed results. Here the intensity of the first order is depicted as a function of sample thickness in the different geometries. The intensity in the HH geometry, in the thickness range 50 to 200 μm, is more than that in the HV geometry [Fig. 4(a)], whereas the intensity in the VH geometry is throughout more than that in the VV geometry [Fig. 4(b)]. This is in accordance with the observed results shown in Fig. 2. Further, Fig. 4(a) shows that around 250 μm the intensity behavior in the HH and HV geometry can get reversed. This explains the contrasting behavior in the HH and HV geometries of the 250 μm sample at 45.5 °C [Fig. 2(b)] and at 50.6 °C (Fig. 3). However, the observed results in VV and VH geometries of the 250 μm sample at 50.6 °C are not in accordance with the computed results shown in Fig. 4(b). Also, our observed results for 23 μm, at all temperatures, show the HH component to be greater than the HV component and this is not in accordance with the result shown in Fig. 4(a). It may be pointed out that the computations shown in Fig. 4 are for one set of material parameters. These parameters are sensitive functions of

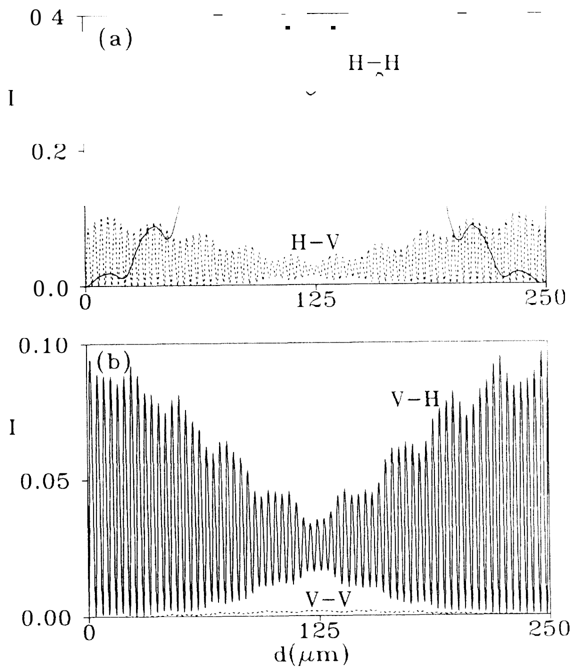

FIG. 4. The normalized intensity I as a function of sample thickness d (μm) for different geometries in the first order. In these computations, the following material parameters of SCE-6 have been used: birefringence =0.18, pitch =5 μm, and tilt angle =18°.

the temperature. It was found that the theory can yield qualitatively all the above observed results by a proper choice of material parameters. Also, the computations show that the RY theory can account for the observed polarization features of the zeroth order as well as those of the higher diffraction orders.

The other interesting feature in Fig. 4 is the appearance of modulations. These modulations in the diffracted intensity can be interpreted as being due to the different orders of scattering. This can be shown by using a perturbation theory [16] where the z-dependent (the propagation direction) part of the dielectric tensor is treated as a perturbation over an effective anisotropic homogeneous medium

In conclusion, we have experimentally studied, lor the first time, the polarization and Intensity fed-tures of the diffraction in the phase grating mode in S_C^*. The observed results are very surprising and interesting and these can be accounted for on the basis of the RY theory.

[1] R. B. Meyer, L. Liebert, L. Strzelecki, and P. Keller, J Phys. (Paris). Lett. **36**, L69 (1975).

[2] N. A. Clark and S. T. Lagerwall, Appl. Phys. Lett **36**, 899 (1980).

[3] L. J. Yu, H. Lee, C. S. Bak. and M. M Labes, Phys. Rev Lett. **36**, 388 (1976).

[4] P. Pieranski, E. Guyon, and P. Keller, J. Phys. (Paris) **36**, 1005 (1975)

[5] S. Garoff and R. B. Meyer, Phys. Rev. Lett. **38**, 848 (1977).

[6] N. M. Shtykov, M. I. Barnik, L. A. Beresnev, and L. M. Blinov, Mol. Cryst. Liq. Cryst. 124. 379 (1985).

[7] J. E. Maclennan. N. A. Clark. M. A. Handschy, and M. K. Meadows, Liquid Crystals **7**, 753 (1990).

[8] D. W. Berreman, Mol. Cryst. Liq. Cryst. 22. 175 (1973)

[9] C. Oldano, Phys. Rev. Lett. **53**, 2413 (1984).

[10] K. Rokushirna and J. Yamakita. J. Opt. Soc. Am. A **4**, 27 (1987).

[11] H. L. Ong. Phys. Rev. A **37**. 3520 (1988).

[12] Ph. Martinot-Lagarde, J. Phys. (Paris), Colloq. **37**, C-129 (1976); K. Kondo, F. Kobayashi, H. Takezoe, A. Fukuda, and E. Kuze, Jpn. J. Appl. Phys. 19, 2293 (1980).

[13] C. V. Raman and N. S. Nagendra Nath. Proc. Indian Acad. Sci. A 2,306 (1935).

[14] K. A. Suresh, P. B. Sunil Kumar, and G. S. Ranganath, Liq. Cryst. **11**, 73 (1992).

[15] K. Rokushima and J. Yamakita, J. Opt. Soc. Am. **73**. 901 (1983).

[16] P. Galatola, C. Oldano. and P. B. Sunil Kumar. J. Opt. Soc. **Am.** A (to be published).

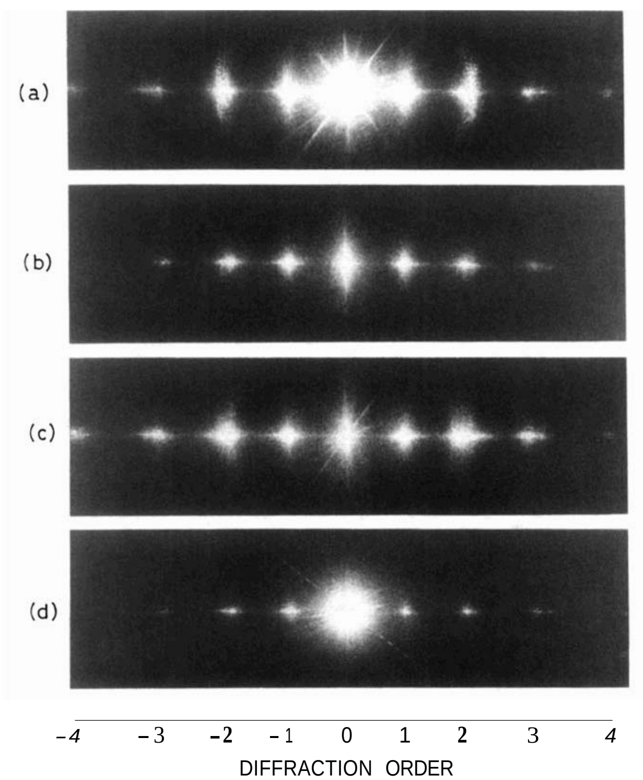

FIG. 1. The photographs of the diffraction pattern of a 50 μm sample at room temperature ($\approx$ 25°C) in (a) HH, (b) *HV*, (c) VH, and (d) *VV* geometries. One may note that in (c) the second order is more intense than the first order. Such effects are characteristic of phase gratings. In S_C*, they are sensitive to temperature.

15 January 1995

OPTICS COMMUNICATIONS

ELSEVIER

Optics Communications 114 (1995) 18–24

Optical diffraction in some Fibonacci structures

Yuvaraj Sah, G.S. Ranganath

Raman Research Institute, Bangalore 560080, India

Received 5 May 1994; revised manuscript received 12 September 1994

Abstract

Optical diffraction from Fibonacci structures has been studied. We find that in a lattice with absorbing elements it is asymmetric. In the diffraction from a phase grating, intense orders cannot always be indexed with a successive pair of Fibonacci numbers. Bragg reflection spectra of multilayers depend on sample thickness and absorption and are different for isomorphic multilayers.

1. Introduction

Since the discovery of quasi-periodic materials by Shechtman et al. [1] the subject has attracted a lot of attention. The pioneering works of Levine and Steinhardt [2], and Socolar and Steinhardt [3] on quasi-periodic tilings have led to many new insights into the structure of such systems. In the beginning, it was only by electron and X-ray diffractions that these structures were studied. But in recent times quasi-periodic gratings and multilayers [4,5] have indeed been made in the laboratory [6,7]. This has led to the study of their optical properties. Self-similarity in the reflection-band [4], localization of light [4,7] and power law transmittance with a critical exponent [6] are some of the interesting features associated with such systems.

In this paper we have worked out the optical properties of some new types of quasi-periodic structures which appear not to have been considered so far. We have confined ourselves to three types of structures viz, amplitude gratings, phase gratings and multilayers. In each case we find some new and interesting effects. In the case of amplitude gratings we have considered optical analogues of quasi-periodic crystals with a Fibonacci sequence in the atomic form factor and interatomic distances. Possibilities of such structures which are accessible in the X-ray region have not been looked into so far. In the case of quasi-periodically stacked multilayers we have addressed ourselves to a quasi-periodic helical stack of birefringent layers such as cholesteric liquid crystals. This is of relevance to the understanding of the Blue phase III which exists in some cholesteric liquid crystals before the structure melts into an isotropic liquid [8,9].

2. Structure of quasi-periodic lattices

We consider a quasi-periodic structure constructed according to a procedure due to Levine and Steinhardt [2]. The Nth lattice point of the quasi-periodic lattice is given by

$$X_N = (N + \alpha + h[hN + \beta])l, \tag{1}$$

where α and β are arbitrary real numbers, h is an irrational number and N is an integer. Here [ ] means that we take only the greatest integral value of the term in-

SSDI 0030-4018(94)00600-8

side the bracket. For $h = 0$ the structure becomes periodic with a spacing l. For $1/h = (\sqrt{5}+1)/2$ the difference $X_{N+1} - X_N$ will be one of the two incommensurate lengths l_1 and l_2 such that $l_2 = (h+1)l_1$. The two lengths l_1 and l_2 occur according to the Fibonacci sequence (FS). For any other value of h we get an entirely different sequence. Changes in the value of α results in the shift of the lattice. Different values of β generate different FSs and these sequences are locally isomorphic [2], i.e., arbitrarily large regions of the two sequences can be made identical.

The standard FS can also be generated using an iterative method [4]. The jth sequence is given by

$$M_j = (M_{j-1}, M_{j-2}), \tag{2}$$

with $M_0 = (S_1)$ and $M_1 = (S_2)$ where S_1 and S_2 are the two distinct elements of the FS. For example $M_2 = (S_2, S_1)$, $M_3 = (S_2, S_1, S_2)$ and $M_4 = (S_2, S_1, S_2, S_2, S_1)$. It is worth mentioning here that in this procedure it is not possible to generate isomorphic FSs.

3. Diffraction pattern

3.1. Amplitude gratings

Optical diffractions in quasi-periodic amplitude gratings have been studied both experimentally and theoretically by Tanibayashi [10]. He found that the diffraction pattern has not only a rich structure but is also self-similar. We consider here two different types of quasi-periodic amplitude gratings not so far considered by others.

The first type of grating is a sequence made up of two slits of widths S_1 and S_2 (which are incommensurate) occuring according to the usual FS, but on a periodic lattice with an edge to edge separation of D, i.e., the sequence of the elements is $S_1, D, S_2, D, S_1, D, S_1, D, S_2, \ldots$. This structure is rather analogous to a one-dimensional periodic crystal with FS in atomic form factors.

In the second type of grating, the slit width S as well as the edge to edge separation D between neighbouring slits occur in a FS, i.e., the sequence is $S_1, D_1, S_2, D_2, S_1, D_1, S_1, D_1, S_2, \ldots$. Also the two slit widths S_1 and S_2, as well as the slit separations D_1 and D_2 are considered to be incommensurate. This is analogous to a one-dimensional quasi-periodic crystal in which atomic form factors and the interatomic distances occur according to a FS.

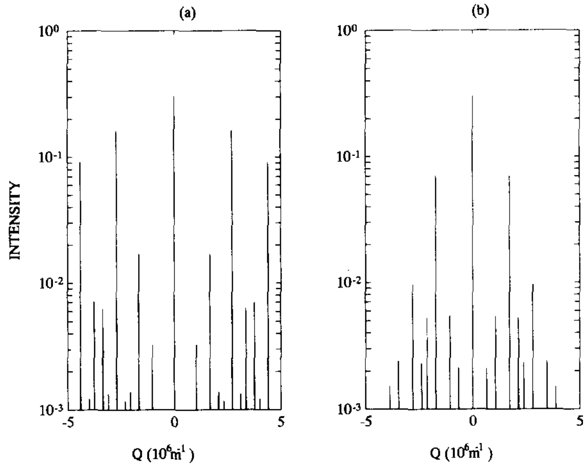

Fig. 1. The diffraction pattern for quasi-periodic amplitude gratings (a) for the sequence $S_1, D, S_2, D, S_1, D, S_1, D, S_2, \ldots$ (b) for the sequence $S_1, D_1, S_2, D_2, S_1, D_1, S_1, D_1, S_2, \ldots$.

The diffraction patterns have been computed in each case for the sequence M_{14}, which has 610 elements. The finite size of the grating did not result in a spurious diffraction pattern, i.e the diffraction pattern remains nearly unchanged, only for any of the 350 or more continuous elements of this sequence. However, for sequences up to M_{10} or for any higher sequence with 100 or less number of continuous elements the pattern is asymmetric. Also each diffraction order is broad. In view of this we calculate the diffraction pattern for first 400 continuous elements of M_{14} sequence. In Fig. 1a we have given the computed pattern obtained in the first type of grating. Here the intensity of different orders is plotted as a function of the scattering wavevector Q, which is related to the angle of diffraction θ and A, the wavelength of light by the relation $Q = (2\pi/\lambda)\sin(\theta)$. For the quasi-periodic medium the diffraction pattern [2,3] has peaks at

$$Q = \frac{2\pi}{l(1+h^2)}(p + hq), \tag{3}$$

where p and q are integers and l is the period of the structure when $h = 0$. The second type of grating results in a diffraction pattern shown in Fig. 1b.

We have also investigated both these cases when either S_1 or S_2 is absorbing, i.e., it is masked with a material with complex refractive index. With S_2 ab-

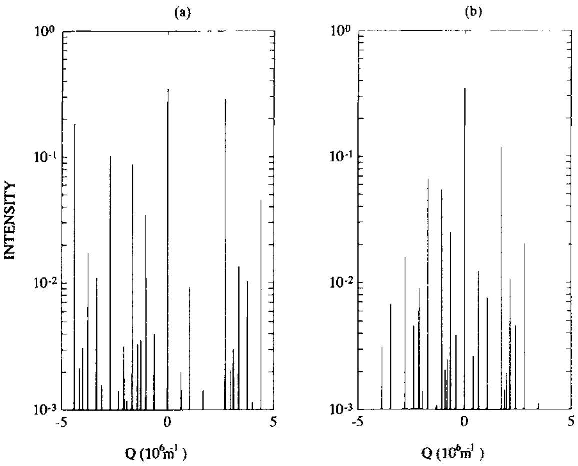

Fig. 2. The diffraction for same gratings with the slit *S2* acting as an absorbing element. The amplitude of transmittance of the slit S_2 is taken to be $(1+i)/\sqrt{2}$.

sorbing, the diffraction pattern has been computed. We find not only some extra orders, but also an asymmetric diffraction pattern. This is shown in Figs. 2a and 2b. We can understand asymmetry in the pattern by appealing to the symmetry of the lattice. For example a periodic lattice with a pair of slits at each lattice point is in general non-centro symmetric and with one of the slits absorbing the diffraction pattern is always asymmetric. This is due to the fact that the absorbing element contributes an extra phase. This results in an asymmetry in the diffraction pattern. This is the optical analogue of an equivalent result in X-ray diffraction from absorbing non-centrosymmetric crystals [11]. It is now well established [2] that Fibonacci sequence is a non-centro symmetric in nature. Hence if it has absorbing elements, it will result in an asymmetric diffraction pattern.

3.2. Phase gratings

Raman and Nath (RN) [12] investigated optical diffraction due to ultrasonic waves in an isotropic medium. When refractive index variations are small we can ignore internal refractions and an incident plane wavefront emerges as a periodically corrugated wavefront. The diffraction pattern can be easily calculated under the two assumptions: (i) wavelength of light is much less than the correlation length of the phase fluctuations on the wavefront, (ii) the magnitude of phase fluctuations is much less than correlation length of the phase fluctations. Mosseri and Bailly [13] considered theoritically RN diffraction from a quasi-periodic structure obtained by superposing two ultrasonic waves of incommensurate wavelengths. This has many peculiar features not found in the classical periodic phase gratings. Recently RN diffraction from a fivefold quasi-periodic structure obtained by superposing five ultrasonic waves in a liquid has also been studied experimentally [14]. It must be remarked that the phase grating effects can also arise in other situations. Two such examples are considered here.

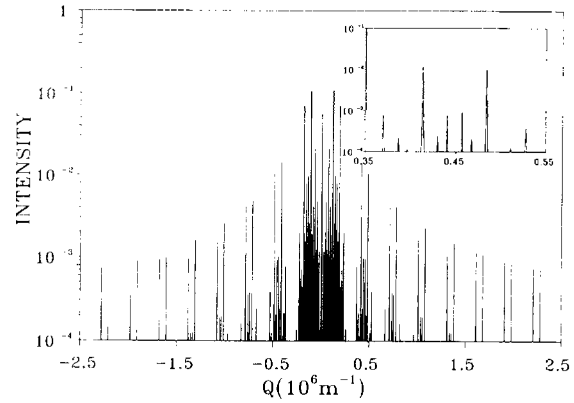

Fig. 3. Diffraction pattern of a step phase grating with step height H_1 and H_2 arranged in a Fibonacci sequence.

3.2.1. Step gratings

Periodic phase gratings involving optical steps are well known [15]. Here we consider periodic gratings but with the optical steps of heights H_1 and H_2 arranged according to the FS: H_1, H_2, H_1, H_1, H_2, H_1, H_2... For an incident plane wavefront both the steps H_1 and H_2 have the same width but different optical paths. We assume H_1 to have a longer optical path length compared to H_2. We use the RN theory to work out the diffraction pattern. In our computations we assume the sample to be uniformly 20 μm thick, but the refractive indices for the steps H_1 and H_2 are 1.58 and 1.5, respectively, and each step has width of 5 μm. Here again the diffraction pattern is found not to be dependent on grating width when the grating has 400 or more elements. This is depicted in Fig. 3. The diffraction pattern is symmetric. All the diffraction orders have same diffraction features. It must be remarked that in the case of normal periodic step gratings with the same number of elements one gets sharp peaks. But in the present structure each diffraction order has a small spread. This spread is due to the fact that each diffraction order has a fine structure (see inset Fig. 3). This fine structure is same in all the orders and is independent of lattice size and persists even when we take many more diffracting elements.

3.2.2. Anisotropic gratings

Phase grating effects also appear in locally anisotropic structures. As an example of such a medium we consider a cholesteric liquid crystal which is optically equivalent to an uniform helical stack of birefringent layers [16,171. In general a plane wavefront of polarised light falling normal to the twist axis emerges as a phase corrugated wavefront resulting in optical diffraction. For the component of the electric vector parallel to twist axis such a phase corrugation will not exist, i.e., diffraction will be absent. We have worked out the diffraction pattern in a quasi-periodic cholesteric medium. We consider the structure to be twisted in a particular direction according to the FS, i.e., two incommensurate but uniformly twisted regions of thicknesses l_1 and l_2 occurring in a FS. Within each such unit we have a uniform helical stack of birefringent layers, with a total twist of 2π. Also $l_1 = (1 + h) l_2$. Here the dielectric tensor is locally uniaxial and gradually rotates along the twist axis but with two incommensurate periods. We assume the incident plane wavefront to fall normal to the twist axis and to be linearly polarised with its azimuth perpendicular to the twist axis. The refractive index for this polarisation varies along the twist axis. At any point the refractive index n_z for this polarisation is given by

$$\frac{1}{n_z^2} = \frac{\cos^2(\theta)}{n_1^2} + \frac{\sin^2(\theta)}{n_2^2}, \tag{4}$$

where 8 is the azimuth of the major axis of the local index ellipsoid whose principle refractive indices are n_1, n_2. Then the emergent wavefront is also linearly polarised with its azimuth perpendicular to the twist axis and it has phase fluctuations resulting in a corrugated wavefront. This leads to optical diffraction. We have shown in Fig. 4 the computed diffraction pattern. It may be mentioned [17] that in a periodic cholesteric in the same geometry the diffraction peaks will occur for the wavevectors $Q = 2\pi(N/l)$, N being an integer.

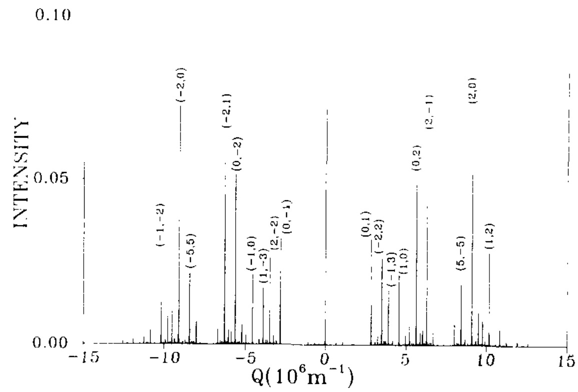

Fig. 4. Diffraction pattern for a quasi-periodic cholesteric medium in the phase grating mode for n_1=1.535, n_2=1.565, sample thickness = 20 μm, A = 0.633 μm and l = 0.2618 μm. We have given the pairs of integers (p, q) only for the intense peaks.

However, the diffraction pattern of a quasi-periodic medium has peaks at Q given by Eq. (3).

It is well known that in a quasi-periodic amplitude grating the intense diffraction peaks occur when p and q are in the ratio of successive Fibonacci numbers [2]. But interestingly in a quasi periodic phase grating we do not find this result. The intensity in any given order is a function of the birefringence of the medium, sample thickness and wavelength.

We can in principle introduce linear dichroism into the system by doping it with solute molecules [18]. Then, generally, the local solute distribution depends on the local twist of the medium and to a good approximation it will be inversely proportional to the twist in the medium. This will lead to a non-uniform absorption in the quasi-periodic cholesteric. In such a non-uniformly absorbing system we get diffraction even for an incident light linearly polarised parallel to the twist axis [19]. This being due to the variations in the magnitude of the amplitude of the emergent wavefront. It is important to note that diffraction in this geometry will be totally absent in a uniformly absorbing periodic or quasi-periodic cholesteric medium.

It should be emphasised that the RN theory does not take into account the internal diffractions inside the medium. Hence the theory is valid only for thin samples or for low birefringent media. For thick samples or for high birefrigent media the magnitude of the phase fluctuations will be very large and one has to use the more rigorous methods which incorporate the internal diffractions [20,21].

3.3. Anisotropic multilayers

Optical Bragg reflections from the quasi-periodic multilayers [4–6] have been studied in systems with optically isotropic layers. We consider here a system with anisotropic layers. The quasi-periodic cholesteric liquid crystal discussed in the previous section is a good example for such a system. The incident light enters the medium along the twist axis. The electromagnetic wave propagation in this medium can be analysed using the 4 x 4 Berreman matrix method [22]. According to this approach a column vector ψ is defined in terms of the electric and magnetic field components

$$\psi = \begin{bmatrix} E_x \\ H_y \\ E_y \\ -H_x \end{bmatrix}.$$

In terms of ψ the Maxwell's equations can be written in the following matrix form

$$\frac{\partial \psi}{\partial z} = \frac{\mathrm{i}w}{c} \Delta(z) \psi, \tag{5}$$

where the matrix $\Delta(z)$ depends on the dielectric tensor. For a periodic medium of period l, the above equation can be solved numerically to get the propagation matrix F which connects the fields at $z = 0$ and the field at $z = l$. Then the propagation matrix for m periods is $(F)^m$. For the quasi-periodic structure we first compute the propagation matrices F' and F'' for the two elements of incommensurate thicknesses l_1 and l_2. Within each of these units the index ellipsoid uniformly rotates through 2π. The net propagation matrix F, for the jth Fibonacci sequence is obtained by multiplying sequentially F' and F'' according to the FS. If ψ_t, ψ_r and ψ_i are the transmitted, reflected and the incident fields then we have the relation

$$\psi_t = F_j(\psi_i + \psi_r). \tag{6}$$

Expressing the reflected and the transmitted fields in terms of the incident field one can calculate the reflectance and the transmittance of the quasi-periodic medium. The net electric field inside the medium is calculated following the procedure of Berreman [22].

We assume a right-handed quasi-periodic medium, with the local principal dielectric constants to be $\epsilon_1 = 2.14$ and $\epsilon_2 = 2.35$. We find that at the normal incidence, the eigenwaves are to a good approximation, right and left circular waves, i.e., they are same as those of a normal cholesteric. The left circular wave always propagates without any attenuation but the right circular wave suffers attenuation, i.e., it gets Bragg reflected. The positions of the Bragg peaks are given by

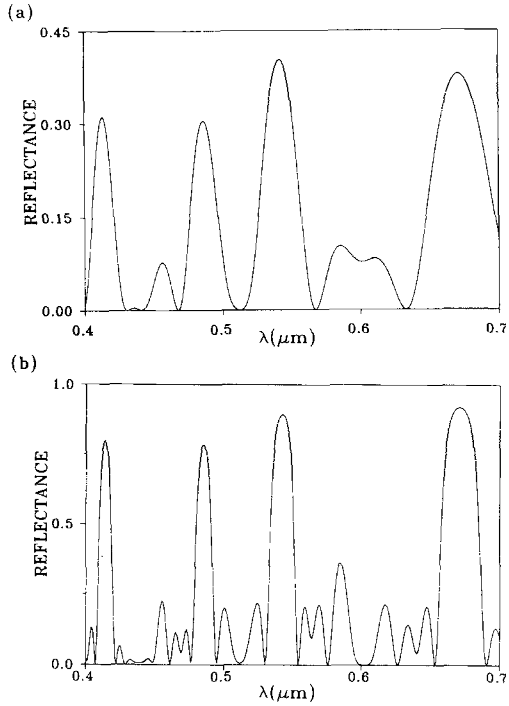

Fig. 5. Reflection spectrum for a quasi-periodic cholesteric medium (a) 10 elements (b) 25 elements.

$$\lambda = \bar{\mu} l(1 + h^2)/(p + qh), \tag{7}$$

where $\bar{\mu}$ is the mean refractive index of the medium and l is the period of the medium when $h = 0$. However, in a periodic structure only one Bragg peak occurs. This will be situtated at $\lambda = \bar{\mu} l$.

Figs. 5a and 5b show the reflection spectra for a quasi-periodic cholesteric with 10 and 25 elements respectively. Interestingly as we increase the number of elements, more and more reflection-bands appear. This can also be seen from the dispersion curves shown in Figs. 6a and 6b for the same structures. One of the interesting properties associated with this medium is the self-similarity [4,5]. This self-similarity is a consequence of a six-cycle mapping for the propagation matrix, i.e., $F_j = F_{j+6}$. We have compared the reflection spectra obtained for F_9 [55 elements] for the region λ = 0.47 μm to 0.56 μm (Fig. 7a) with that

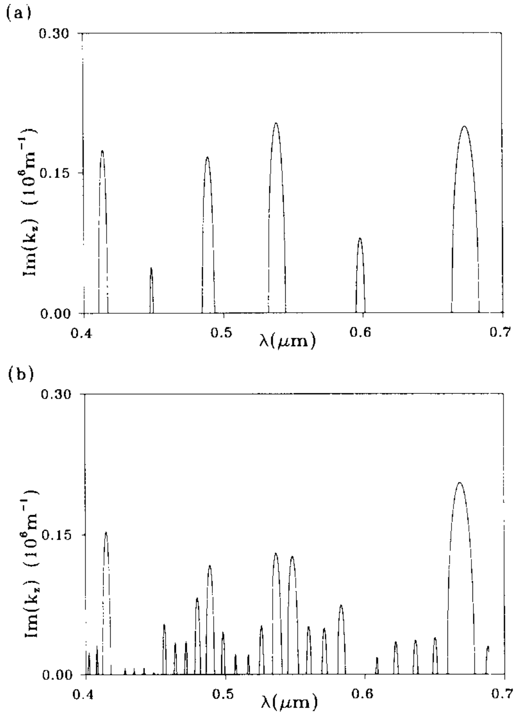

Fig. 6. Dispersion curve for a quasi-periodic cholesteric medium (a) 10 elements, (b) 25 elements. Here k_z is the wavevector inside the medium.

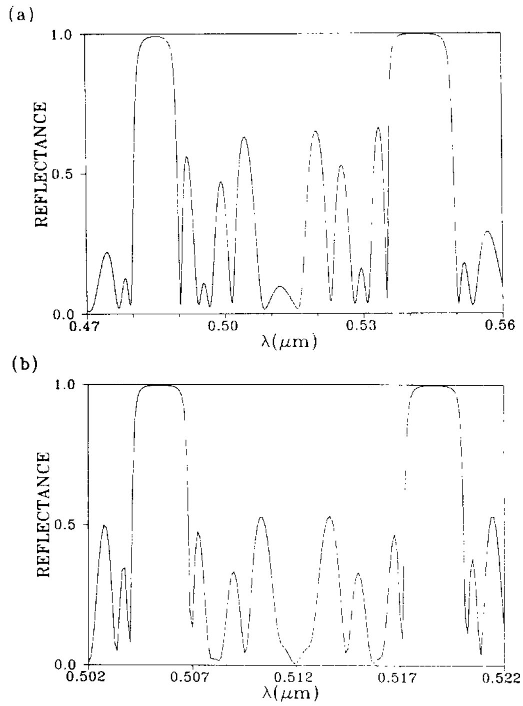

Fig. 7. Comparison of the reflection spectrum of (a) 55 elements with (b) 233 elements in the quasi-periodic cholesteric medium. One may note the self-similarity between the two.

of F_{12} [233 elements] (Fig.7b) for the region A = 0.5 μm to 0.525 μm . We can clearly see that in this case there is a self-similarity between the two reflection spectra. It must be noticed that the transmission spectra is complimentry to reflection spectra.

We have also worked out the nature of the standing waves in the Bragg-bands. As in normal cholesterics here also the net E field of the standing wave is a linear vibration, with E ‖ H. The azimuth of the E field rotates by $\pi/2$ as we move from one edge of a reflection-band to its other edge. In any given reflection-band the azimuth of E uniformly rotates as we move along the twist axis, with a constant pitch. This pitch is different in different reflection-bands. Also the intensity of the E field attenuates by different amounts in different reflection-bands, but in every band the decay is non exponential. This is in contrast to the exponential decay found in normal cholesterics [19].

The effect of dichroism can be easily worked out. In Fig. 8 we have given the reflection spectra for 25 linearly dichroic birefringent elements. Comparing this with the reflection curve shown in Fig. 5b, for an identical non-absorbing sequence, we find that many of the reflections of the non-absorbing multilayer stack are absent in the absorbing case. Also in this case the transmission spectra is not complementry to the reflection spectra.

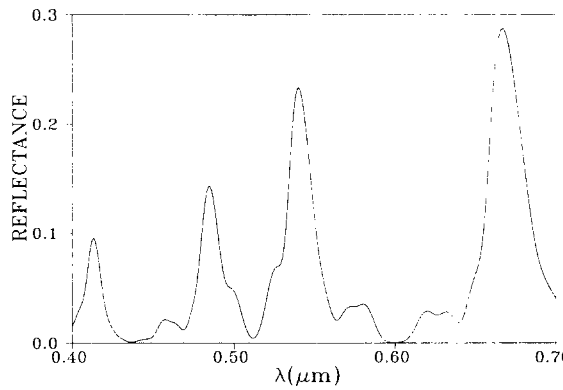

Fig. 8. Reflection spectrum for an absorbing 25 elements thick quasi-periodic cholesteric meduim. Here Im(ϵ_1) = 0.0063 and Im(ϵ_2) = 0.063. This may be compared with Fig. 5b which represents the reflection spectrum for an identical multilayer without absorbtion.

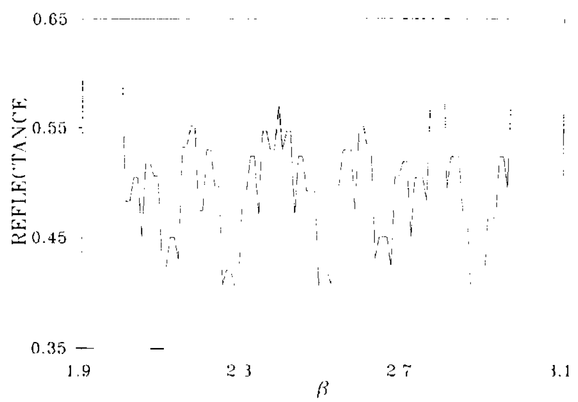

Fig 9 Intensity of Bragg reflection at $\lambda = 0.505$ μm as a function of β for 233 elements

3.4. Effect of β on diffraction

We have already stated that a change in β leads to an isomorphic FS. In both the amplitude and phase gratings the diffraction pattern obtained for different isomorphic FSs have peaks at same positions but the phases of the corresponding orders are different. This phase is a function of β. However in the case of a multilayered medium in the Bragg reflection mode which incorporates multiple reflections, we get a very interesting result. The intensity of some of the Bragg reflections get altered as β changes. This is shown in Fig. 9 for a particular Bragg-reflection.

4. Conclusions

We have studied optical diffraction in amplitude gratings, phase gratings and multilayers with a Fibonacci sequence of elements. The diffraction patterns from quasi-periodic gratings are rich and can also be asymmetric if one of the two elements of the Fibonacci sequence is absorbing. Though diffraction peaks from quasi-periodic phase gratings can be indexed with two integers, they need not be successive pair of Fibonacci numbers for intense orders. At normal incidence, several Bragg-bands exist in the quasi-periodic Fibonacci multilayer structure, the number of these bands increases with increasing thickness of the structure. Also absorption considerably alters the reflection spectra. The electric field inside the medium, for the Bragg reflected mode, has a non-exponential decay. Though isomorphic amplitude and phase grating give identical diffraction patterns isomorphic multilayers have different reflection spectra.

Acknowledgements

Our thanks are due to K. A. Suresh, P.B. Sunil Kumar and N. Andal for discussions. Thanks are also due to the referee for suggestions.

References

[1] D. Shechtman, I. Blech, D. Gratias and J.W. Cahn, Phys. Rev. Lett. 53 (1984) 1951.
[2] D. Levine and P.J. Steinhardt, Phys. Rev. B 34 (1986) 596.
[3] J.E.S. Socolar and P.J. Steinhardt, Phys. Rev. B 34 (1986) 617.
[4] M. Kohmoto, B. Sutherland and K. Iguchi, Phys. Rev. Lett. 58 (1987) 2436.
[5] A. Latgé and F. Claro, Optics Comm. 94 (1992) 389.
[6] L. Chow and K.H. Guenther, J. Opt. Soc. Am. A 10 (1993) 2231.
[7] W. Gellermann, M. Kohmoto, B. Sutherland and P.C. Taylor, Phys. Rev. Lett. 72 (1994) 633.
[8] R.M. Hornreich and S. Shtrikman, Phys. Lett. A 115 (1986) 451.
[9] D.S. Rokhsar and J.P. Sethna, Phys. Rev. Len. 56 (1986) 1727.
[10] M. Tanibayashi, J. Phys. Soc. Japan 61 (1992) 3139.
[11] R.W. James, The optical principles of the diffraction of X-rays (Bell, London, 1948).
[12] C.V. Raman and N.S. Nagendra Nath, Proc. Indian Acad. Sci. A 2 (1935) 406.
[13] R. Mosseri and F. Bailly, J. Phys. I France 2 (1992) 1715.
[14] F.M. de Espinosa, M. Toms, G. Pastor, M.A. Muriel and A.L. Mackay, Europhys. Lett. 21 (1993) 915.
[15] A. Sommerfeld, Optics, Lecture on theoretical Phys. Vol. IV (Academic Press, 1949).
[16] S. Chandrasekhar and J.S. Prasad, Physics of the solid state, ed. by S. Balakrishna (Academic Press, 1969).
[17] K.A. Suresh, P.B. Sunil Kumar and G.S. Ranganath, Liq. Crystals 11 (1992) 73.
[18] E. Sackmann and L. Voss, Chem. Phys. Lett. 14 (1972) 528.
[19] P.B. Sunil Kumar and G.S. Ranganath, J. Phys. II, 3 (1993) 1497.
[20] K. Rokushima and J. Yamakita, J. Opt. Soc. Am. 73 (1983) 901.
[21] P. Galatola, C. Oldano and P.B. Sunil Kumar, J. Opt. Soc. Am. 11 (1994) 1332.
[22] D.W. Bemman, J. Opt. Soc. Am. 62 (1972) 502.